LIMNOLOGY
and
OCEANOGRAPHY

Detritus-hosted methanogenesis sustains the methane paradox in an alpine lake

Maciej Bartosiewicz [1,2]* Jessica Venetz,[1] Saskia Läubli,[1] Oscar Sepúlveda Steiner [3,4]
Damien Bouffard,[3,5] Jakob Zopfi,[1] Moritz F. Lehmann[1]

[1]Aquatic and Stable Isotope Biogeochemistry, Department of Environmental Sciences, University of Basel, Basel, Switzerland
[2]Institute of Geophysics, Polish Academy of Sciences, Warsaw, Poland
[3]Department of Surface Waters—Research and Management, Eawag, Swiss Federal Institute of Aquatic Science and Technology, Kastanienbaum, Switzerland
[4]Physics of Aquatic Systems Laboratory, Margaretha Kamprad Chair, Institute of Environmental Engineering, École Polytechnique Fédérale de Lausanne, Lausanne, Switzerland
[5]Institute of Earth Surface Dynamics, University of Lausanne, Lausanne, Switzerland

Abstract

Accumulation of methane in oxic waters of lakes and the ocean has been widely reported. Despite the importance for the greenhouse gas budget, mechanistic controls of such "methane paradox" remain elusive. Here, we use a combination of CH_4 concentration and isotopic ($\delta^{13}C_{CH_4}$, δD_{H_2O} and $\delta^{18}O_{H2O}$) measurements, plankton incubations and microbial community assessments to demonstrate the existence of the methane paradox in oxygenated waters of a meromictic lake (Lake Cadagno, Switzerland). Following mass dynamics using water isotopes, we exclude the possibility that the accumulation of CH_4 at the thermocline results solely from lateral transport. Interannual variability in the magnitude of the methane paradox (between 0.5 and 5 μmol L^{-1}) is associated to stratification patterns, changes in zooplankton biomass and planktonic detritus accumulation along density gradients, as well as fluctuating microbial cell numbers. The links between hydrodynamic conditions, aggregation of planktonic detritus and its microbiome, as well as the accumulation of CH_4 in the water column are further supported by high-resolution echo-sounder measurements revealing backscatter maxima at the top of the thermocline, where detritus is effectively trapped, and by oxic incubations showing that CH_4 is produced in zooplankton detritus (0.046 nmol L^{-1} to 0.095 CH_4 mg dry mass L^{-1} d^{-1}). Our results also show that detritus-hosted methanogenesis is stimulated through the addition of methylphosphonate, suggesting that zooplankton-associated microbiomes exploit organic phosphorus compounds to release CH_4. Understanding the variability of the methane paradox in relation to changing hydrodynamics and plankton communities will be crucial to predict the future role of lakes in the global methane budget.

*Correspondence: maciej.bartosiewicz@igf.edu.pl

Additional Supporting Information may be found in the online version of this article.

Atmospheric levels of methane (CH_4) increased by 150% since the beginning of the industrial era, and contribute as much as 20% to the planetary warming (Kirschke et al. 2013). Understanding the processes controlling production and potential emission of this potent greenhouse gas (GHG) to the atmosphere is therefore of crucial importance for predicting trajectories of future climate change and related ecosystem feedback effects. Methanogenesis, traditionally regarded as a strictly anaerobic process performed by *Archaea*, is responsible for most of the biogenic CH_4 production (Ferry 2012) and, as a consequence, the research focus was traditionally on anoxic sections of wetlands, as well as anoxic marine and lacustrine sediments, with only little attention given to processes generating CH_4 under oxic conditions (Grossart et al. 2011). However, already early work evidenced persistent CH_4 oversaturation in

well-oxygenated ocean waters (Traganza et al. 1979) and related this phenomenon, which has been referred to later as the "global methane paradox" (Karl and Tilbrook 1994), to plankton activity. The methane paradox appears as an important component of the global GHG budget, since CH_4 accumulating in near-surface waters is often directly released to the atmosphere and thus contributes largely to aquatic CH_4 emissions (Tang et al. 2016).

Over the past decade, numerous marine and freshwater studies expanded the existing evidence for the accumulation of methane in oxygenated waters ("methane paradox") and its production under oxic conditions by various microorganisms and through different biotic and/or abiotic processes (i.e., Tang et al. 2014; Zhang and Xie 2015; Bižić et al. 2020). Potential CH_4 generation in oxygenated waters was associated to: (1) organic matter (OM) processing within anoxic microsites (Sasakawa et al. 2008), (2) zooplankton and phytoplankton activity (de Angelis and Lee 1994; i.e., Stawiarski et al. 2019), (3) presence of plankton associated methanogens (Grossart et al. 2011), and (4) cyanobacterial exploitation of methylated nutrients (Teikari et al. 2018). Most recently, it was also shown experimentally that cyanobacteria can produce CH_4 during photoautotrophic conversion of CO_2 (Bižić et al. 2020). Alternative, physical, explanations for the methane paradox include advective and lateral transport of CH_4-rich waters from benthic production sites (Encinas Fernández et al. 2016), or the dissolution of CH_4-rich bubbles along density gradients (McGinnis et al. 2006). In situ aerobic production and transport processes are not mutually exclusive as explanations for the methane paradox and have been shown to play a role in the CH_4 and carbon budgets of multiple lakes (DelSontro et al. 2018*a*). Nonetheless, while CH_4 transport from the littoral zone may be relatively important in shallow and coastal waters, enhanced OM processing associated to planktonic production and degradation of planktonic biomass will likely play a more important role in the open ocean and in lakes with relatively small littoral zones, or reduced vertical exchange (i.e., meromixis).

Both actively feeding zooplankton and associated planktonic detritus (i.e., fecal pellets, carcasses, molts) have been recognized as anaerobic micro-hot spots in lakes (Glud et al. 2015). Methane production in zooplankton may result from classic methanogenesis within the digestive tracts during feeding (Schmale et al. 2018). Alternatively, zooplankton-associated CH_4 production may be related to methanogenesis in anoxic micro-niches within suspended particular matter, or to the decomposition of methylated compounds by bacteria (i.e., Repeta et al. 2016). Regardless of the exact mechanism, one can anticipate that the accumulation of CH_4 occurs along strong density gradients, where planktonic detritus ("marine" or "lake-snow", Grossart and Simon 1993) persists for days or even weeks due to reduced motion and turbulent fluxes (Kirillin et al. 2012). The magnitude of methane accumulation is likely to depend on the import and aggregation of planktonic OM at

a specific depth in the water column (Oremland 1979), which itself is controlled by multiple factors such as inputs of allochthonous material, autotrophic production, turbulent mixing, phenology of the zooplankton community, and their swarming behavior (Ambler 2002), as well as on the composition of the planktonic detritus and associated microbiomes.

The direct relationship between CH_4 production in oxic waters, the interannual changes in the input of OM, as well as the strength of stratification in lakes has not been demonstrated before. Understanding these links, however, seems to be of particular importance in the light of future climate change effects and synergies related to decreasing transparency and stratification of lakes (Leech et al. 2018). These effects will influence, and most likely enhance, thermal gradients and water-column stability (Bartosiewicz et al. 2019; Woolway and Merchant 2019), and in turn decrease the sinking rates of organic detritus in the upper water column. Then, within thinner but warmer epilimnia, terrestrial OM-supported zooplanktonic biomass is likely to increase (Tanentzap et al. 2017) as more organic substrates will be retained within a steeper temperature gradient at the top of the thermocline. The localized enrichment of nutrients and carbon along subsurface density gradients will represent an excellent feeding-ground for zooplankton and support the activity of detritus-associated methanogens further enhancing CH_4 production in oxygenated waters.

In this work, set within the well-studied ecosystem of meromictic Lake Cadagno (Switzerland, Del Don et al. 2001), we used an interdisciplinary approach to test whether, and to what extent, CH_4 accumulation in oxic waters can be related to zooplankton distribution and the retention of planktonic detritus at the thermocline. For this purpose, we performed field measurements to (1) characterize the spatiotemporal variability of CH_4 in the lake over three consecutive summers with contrasting hydrodynamics and changes in water column stratification patterns, (2) to investigate temporal changes in zooplankton communities, and (3) to follow the possible origin of the observed methane paradox using stable isotope tracing. We further performed oxic incubation experiments to test whether CH_4 is indeed produced by active zooplankton or derives from planktonic detritus, and we characterized the microbiome associated to the methane paradox and to zooplankton detritus, in order to verify the potential of the zooplankton-associated microbiome to produce CH_4 from organic phosphorus compounds. Our combined field and experimental research sheds new light on the mode and importance of "aerobic methanogenesis" in lakes, as well as the mechanisms underlying its temporal fluctuations.

Methods

Study site and sampling campaigns

Lake Cadagno (max depth = 21 m; mean depth = 9.3 m) is a crenogenic meromictic lake located in the southern part of
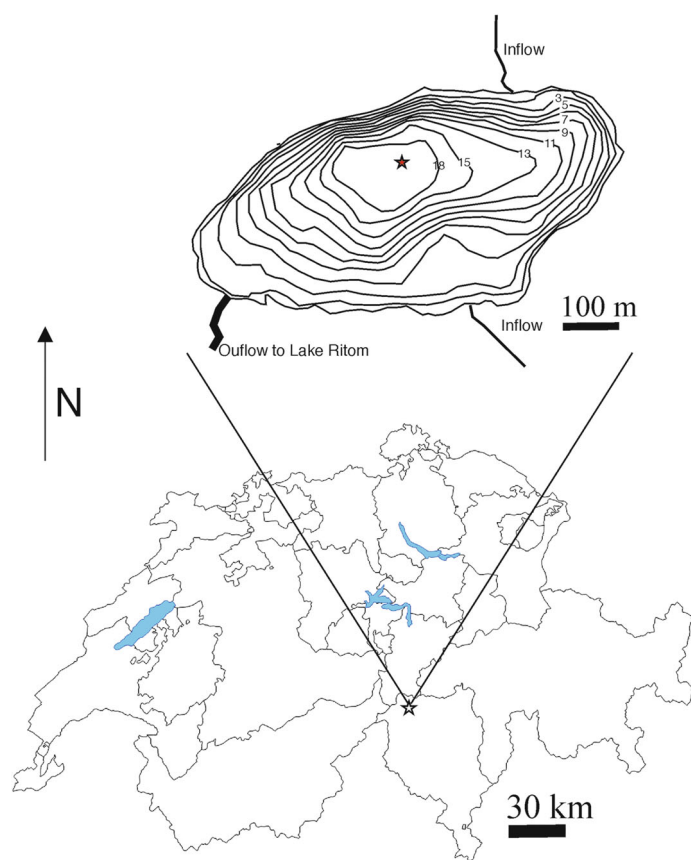
Fig. 1. Location and bathymetry of Lake Cadagno (Ticino, Switzerland). The red star indicates the sampling station on the lake.

the Swiss Alps (Fig. 1). The lake has a surface area of 2.61×10^5 m^2, with a littoral zone (< 2 m deep) of about 1.7×10^4 m^2. Due to the infiltration of subaquatic spring waters that percolate through gypsum-rich dolomites in the catchment, Lake Cadagno bottom waters contain high concentrations of dissolved sulfate (1.5 mmol L^{-1}), sulfide (up to 300 μmol L^{-1}), carbonate, calcium, and magnesium. The water column is characterized by a strong physicochemical gradient (i.e., chemocline) at mid-water depths, (12–13 m) separating the high-salinity (up to 250 mg L^{-1}), euxinic monimolimnion from the aerobic mixolimnion. Phototrophic sulfur bacteria create a thick layer of highly turbid water along the chemocline (13–15 m) of the lake. Sediment pore waters (> 3 mmol L^{-1}) and bottom waters (up to 15 μmol L^{-1}) are rich in CH$_4$, but essentially all of the biogenic CH$_4$ is oxidized first in the sediments (Schubert et al. 2011; Su et al. 2020) and then in the water column (Milucka et al. 2015).

During multiple water column sampling campaigns between July 2016 and August 2018, we have monitored the physicochemistry and CH$_4$ biogeochemistry in the lake, as well as changes in zooplankton community structure. In addition to monthly samplings during the ice-free periods, in order to investigate potential intraday fluctuations of the

methane paradox and potential short-term environmental controls, we also determined fluctuations in the biogeochemistry and hydrodynamics over a full diurnal cycle (30 h) in August 2017, when samples were taken at 6-h intervals. Meteorological data (wind speed, rainfall) for the study region were extracted from the 1 km grid COSMO-1 data (MeteoSwiss; https://www.meteoswiss.admin.ch/weather/warning-and-forecasting-systems/cosmo-forecasting-system.html).

Physicochemistry and stable isotope analysis

Profiles of temperature, conductivity, oxygen, and turbidity were measured using a Yellow Spring Instruments probe during the open water period (June–September) throughout 2016–2018. Surface temperature and thermocline depth were determined from RBR-*solo* thermistor chains installed during ice-free periods of the three analyzed years. During the sampling campaign in 2017, we deployed the Nortek Signature 1000 Acoustic Profiler in echo-sounding mode (1000 kHz) to monitor biomass-induced changes in acoustic backscatter. The device was set up to scan the whole water column at a 5-cm vertical resolution. We estimated dissipation-scale turbulence and vertical diffusivity from measurements performed with a Vertical Microstructure Profiler (VMP-500; Rockland Scientific International). Details of these microstructure measurements and their processing are presented in Sepúlveda Steiner et al. (2019, 2021). Using this detailed dataset, we were able to monitor the evolution of the thermal structure of the upper water column, identify the location of turbid layers, and quantify the level of turbulent diffusion within layers distinguished by the accumulation of planktonic detritus and bacteria. On each occasion, we also collected discrete water samples at the deepest site of the lake (Fig. 1) with a 2 L Niskin bottle at 1-m sampling intervals between the surface down to the redox transition zone (0–14 m). Samples for dissolved CH$_4$ concentration and carbon isotopic (^{13}C/^{12}C) measurements were immediately distributed into triplicate 120 mL serum bottles, and killed with 5 mL of 20% NaOH. At each sampling depth, an aliquot of 2 mL of lake water was syringe-filtered (0.2 μm) and collected into acid-cleaned glass vials for the analysis of water stable isotope ratios (D/H; ^{18}O/^{16}O). During the samplings in July and August 2017, and between June and August 2018, we also collected water samples in the littoral zone for CH$_4$ concentration and carbon isotopic measurements, as well as stable water isotope analyses. Methane oxidation rates (MOx) were determined in quadruplicates from ex situ incubations of water samples with trace amounts of ^{14}C-labeled methane, as described in Steinle et al. (2015) based on a previously described method (Reeburgh et al. 1991).

Upon return to the laboratory, for CH$_4$ concentration measurements, a 20 mL headspace was created in each of the serum bottles with He gas (CarbagGas, 5.0), and samples were allowed to equilibrate prior to analysis using a gas chromatograph equipped with a flame ionization detector (GC-FID; SRI Instruments). For δ^{13}C-CH$_4$ analyses, headspace aliquots

(1–3 mL) were transferred to pre-evacuated 12 mL Exetainers (Labco Scientific) and diluted with high-purity He (6.0) to yield approximately 500 nmol of CH_4. The CH_4/He gas mixture was then analyzed using an isotope ratio mass spectrometer with preconcentration unit (PreCon-IRMS Delta V Advantage; Thermo Fisher Scientific). Water isotope ratios were analyzed by laser absorption spectroscopy using a liquid–water isotope analyzer. Stable carbon and water (hydrogen and oxygen) isotope ratios are reported in the conventional delta (δ) notation as per-mil deviation (‰) with respect to V-PDB and V-SMOW standards, respectively. The $\delta^{13}C$ measurements were calibrated using standard methane/synthetic-air mixtures (CB11010: $\delta^{13}C = -36.03‰$ and CB11117: $\delta^{13}C = -58.03‰$; provided by J. Mohn, EMPA Dübendorf). For the calibration of δD and $\delta^{18}O$ measurements, we used V-SMOW (δD = 0‰, $\delta^{18}O = 0‰$), GISP (δD = −189.5‰, $\delta^{18}O = -24.76‰$), and SLAP (δD = −427.5‰, $\delta^{18}O = -55.5‰$) international standards. Analytical reproducibility based on replicate sample and standard analysis is $\pm 0.2‰$ for $\delta^{13}C$, and ± 0.8 and ± 0.1 for δD, and $\delta^{18}O$, in CH_4 and in H_2O, respectively.

Enumeration of zooplankton, bacteria, and planktonic detritus

Samples for zooplankton counting and identification were collected with a 5 L Niskin bottle, and concentrated to 20 mL directly on the boat using a 20 μm mesh plankton net. Concentrated zooplankton was killed with 20% formalin (0.5% final solution for 1 h), then rinsed thoroughly in tap water, and stored in 70% ethanol. Samples were kept at 4°C until microscopic analysis. Taxonomic identification was carried out to the genus level. The counting of identifiable zooplankton-detritus particles was done by visual enumeration of empty carapaces and large fragments of exoskeletons. Whenever possible, the postmortem morphological changes were used to distinguish between in situ dead animals from those that were killed with formalin (Sampei et al. 2009; Tang et al. 2014). Unconcentrated lake water samples for microbial cell counts were collected into 4 mL cryovials, fixed with 20% formalin (final concentration of 0.2%), snap-frozen in liquid N_2, and stored at −80°C until flow-cytometric analysis (BD Accuri C6 Plus) after a double-staining procedure (SYBR-Green and propidium iodide) allowing us to distinguish between dead and vital cells (Falcioni et al. 2008).

Incubation experiments

A first series of incubation experiments was carried out with zooplankton, hand-picked from a water sample collected at 5–7 m depth. At the beginning of the experiments, 20 similarly sized *Daphnia* sp., *Bosmina* sp., *Cyclops*, or Nauplii, respectively, were transferred to individual 120 mL serum bottles filled with 100 mL of sterile-filtered lake water (0.2 μm). For the control treatment we incubated sterile-filtered lake water only. Each treatment was replicated five times. Animals were incubated for 10 d at room temperature and were fed with

algal food solution (*Nanochloropsis limnetica*) every second day. During the experiment, oxygen concentration was monitored (in one of the replicates for each treatment) using a fiber-optic oxygen meter (PICO2; PyroScience) and optode sensor spots, confirming that O_2 concentrations never dropped below 80% saturation. No case of mortality was observed among incubations with adult animals, yet *Nauplii* molted two to three times during this experiment. Dissolved CH_4 was monitored by subsampling 0.5 mL of the headspace gas (replaced with synthetic air) at several timepoints over the course of the experiment, and analysis of the headspace gas by GC-FID. Aqueous CH_4 concentrations were recalculated according to Henry's Law.

In the second set of experiments, we have collected and incubated different amounts of zooplankton detritus. This was done by concentrating planktonic material (*see* Fig. S1) from 3, 6, and 8 L of lake water collected at 7 m water depth in June 2018 with a 20 μm plankton net, and effectively killing them with heat (37°C for 10 min; *see* Elliott and Tang 2009). The underwater Plankton Camera (Orenstein et al. 2020, curtesy of F. Pomati, EAWAG) was used in Lake Cadagno to confirm that the detritus accumulating within the thermocline (6–8 m) and collected on the 20 μm plankton net during our experiment consisted mostly of zooplankton remains (Fig. S1). Zooplankton detritus was further concentrated by centrifugation (20 min at 400 RCF). Concentrates were treated for 10 s in an ultrasonic bath, and the suspension transferred (10 mL of concentrated detritus per replicate, five replicates per treatment) to 120 mL vials filled with 90 mL of 0.2 μm-filtered lake water. Control incubations consisted of sterile-filtered lake water. Half of the serum bottles were spiked with 200 nmol L^{-1} of C-isotopically distinct methylphosphonate (MPn; $\delta^{13}C$ of $101 \pm 0.5‰$, $n = 5$), a simple one-carbon phosphorous compound. The remaining zooplankton detritus was collected onto a precombusted and preweighted GFF filter for biomass and carbon content assessment. During the experiment, at different time intervals, the air headspace was sampled for CH_4 concentration measurements as described above, and dissolved oxygen was continuously monitored with the optode sensor to verify that all incubations remained oxic (> 80% saturation), regardless of the detritus concentration. In addition, samples for enumeration of microbial cells were collected after the experiment and analyzed as described above for lake water.

Microbial communities in water-column and experimental samples

For DNA extraction, unfiltered water samples (1 L) were collected at discrete depths (0.5, 5, 7 m) in August 2018 and kept ice-cooled during transport to the laboratory. Upon arrival at the home laboratory, the samples were filtered onto 20- and 2.7-μm filters, and the collected material was transferred from these filters into sterile-filtered lake water. Water with the different size fractions (i.e., > 20, 20–2.7, and 2.7–0.2 μm) was

then filtered onto 0.2 μm polycarbonate membrane filters (Whatman) and immediately frozen at -80°C. In the same way, biomass was collected from experimental samples after the incubation experiment for the control, and from the MPn-amended and unamended treatments. All filters with concentrated biomass were extracted using the FastDNA SPIN Kit for Soil (MP Biomedicals) and 30 s of bead-beating at maximum intensity with a Precellys 24 cell disruptor (Bertin Technologies). The V4 and V5 regions of the 16S rRNA gene were amplified using primers 515F-Y and 926R (Parada et al. 2016). Sequencing of amplicons was performed at the Genomics Facility Basel (D-BSSE; ETHZ/University of Basel) on an Illumina MiSeq with the 2 × 300PE protocol (600 V3 kit). Initial quality control of sequence reads and bioinformatic treatment was done at the Genetic Diversity Center (ETHZ) using the pipeline tools, versions, and parameters described in detail elsewhere (Su et al. 2020). Sequences were clustered into OTUs using a 97% sequence similarity threshold (Edgar 2013) and taxonomically assigned with Syntax (Edgar 2016) and the SILVA SSU reference database (https://www.arb-silva.de/documentation/release-128/) (Quast et al. 2013). The raw sequences have been deposited at NCBI under the Bioproject number PRJNA743306 (Accessions: SAMN20009058–SAMN20009063). In order to verify the taxonomy of candidate 16S rRNA gene sequences of methanogens a phylogenetic tree of the archaeal sequences was generated using RAxML (Stamatakis 2014) and a general time-reversible (GTR + Gamma) nucleotide substitution model. In the course of this analysis, and subsequent nucleotide sequence search using Blastn, eight OTUs were identified as 18S rRNA gene sequences wrongly assigned to Archaea (> 95–97% sequence similarity to Amoebozoa of the Vannellidae family), and have been removed from the dataset. Sequences with ambiguous phylum-level annotation as well as sequences of chloroplasts and mitochondria were also removed prior to any further analysis using Phyloseq v1.37 (McMurdie and Holmes 2013) in the R environment (version 4.1.0; R Core Team 2014). The cleaned dataset consisted of six samples with 39,882 to 288,885 reads per sample, clustered into 1554 OTUs. Alpha diversity measures (Chao1 richness estimator, Shannon–Wiener index) were calculated using Phyloseq. For the between-sample (beta-)diversity, sequence data have been rarefied to even depth (1011 OTUs remaining), and Bray–Curtis dissimilarities were computed and ordinated by principal coordinate analysis (PCoA). Permutational multivariate analyses of variances (PERMANOVA) were computed using the adonis function in the R package vegan (Oksanen 2020) with "treatment" (+MPn/−MPn) and size "fraction" (0.2–2.7, 2.7–20, > 20 μm) as factors. The abundance of methanogens in specific samples was determined by qPCR on the mcrA gene using the mcrIRD primers (1 μmol L^{-1} final conc.) of Lever and Teske (2015). qPCR reactions of 20 μL were performed using the SensiFAST SYBR No-ROX Kit (Bioline) on a Mic (Magnetic Induction Cycler) real-time PCR machine (Bio Molecular

Systems, Inc). An initial denaturing step of 95°C for 3 min was followed by 50 cycles of 5 s at 95°C, 10 s at 56°C, and 22 s at 72°C. The specificity of the amplification was assessed by examining the melting curves from 72°C to 95°C, and additional agarose gel electrophoresis. The calibration curve was generated using 10-fold dilution series of pGEM-T Easy plasmid DNA (Promega) carrying a single copy of the target gene.

Statistical analyses

Assessment of differences in the zooplankton community structure and isotopic composition of CH$_4$ between years and between zones within the lake was performed using one-way ANOVA. Comparison of the isotopic (O and H) composition of different water mases was done using ANOVA on ranks followed by a Dunn's test, and differences between experimental treatments were assessed with a two-way ANOVA. Relationships between zooplankton numbers and detritus abundance to CH$_4$ in the water column and during experimental incubations were validated using regression analysis. Whenever required, tests were performed on Ln-normalized data in Statistica 14 software (TIBCO).

Results

Meteorological conditions and water column stratification

The summer in 2018 was the warmest among the studied years, with an average surface water temperature (17.9°C) more than 1°C higher compared to the other years (i.e., 16.6°C in 2016 and 16.3°C in 2017). The summer of 2018 was also drier than the summers of 2017 or 2016, respectively, and did not experience any cold storm events as observed in July and August of the two previous years (Fig. 2A and heat budget in Fig. S2). In contrast, 2017 was relatively rainy, with a total precipitation of 591 mm, as compared to 420 mm in 2016 (most of the difference in September) and only 322 mm in 2018. Intense rainfalls during summer 2017 were accompanied by occasionally strong winds and gusts reaching 20 m s^{-1}. Overall, however, the cumulative wind energy in 2017 was lower than either in 2016 or 2018 (Fig. 2A). While during all years the upper water column (12 m) of the lake was stably stratified between June and August, some interannual differences were nonetheless observed. For instance, the thermocline was located higher up in the water column throughout the summer of 2018 (Fig. 2B). Moreover, a relatively strong storm event in August 2017 significantly affected the thermal structure of the water column by lowering the upper thermocline from between 5 and 6 m to between 7 and 8 m.

The seasonal pattern of the water-column density stratification controls the level of vertical turbulent diffusive flux (e.g., of O$_2$), and exerts an important constraint on the distribution of detrital particles in the water column. Hourly microstructure profiles between 28 and 29 August 2017 revealed
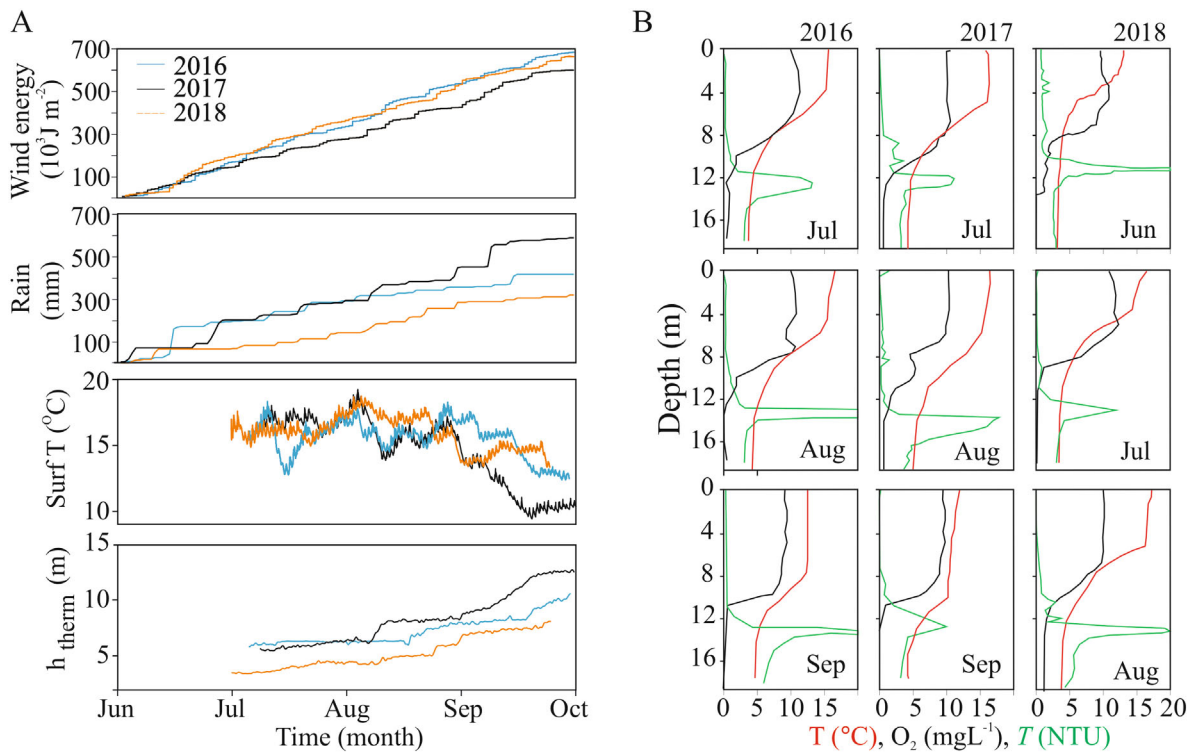
Fig. 2. (**A**) Maximum wind speeds (max. *U*) and seasonal rainfall over Lake Cadagno, evolution of the surface water (0.5 m) temperatures and thermocline depth (*h*), and (**B**) distribution of water-column temperature, oxygen concentrations and turbidity (relative units) between July 2016 and August 2018.

that turbulent diffusivities in the upper layer decreased from $\sim 10^{-3}$ m^2 s^{-1} near the surface down to molecular diffusivity levels at the thermocline (Fig. 3A). Strong stratification is indicated by a local buoyancy frequency (N^2) maximum of 4×10^{-3} s^{-2}. The differential meteorological forcing described above (i.e., strength of the wind shear affecting water column stability and turbulent diffusivity) seemed to be associated to subtle changes in the oxygen zonation during 2018 and 2016, compared to 2017, as indicated by the difference between the surface and mid-water column oxygenation (Fig. 2). Interestingly, in August 2016 and 2017 the oxygen concentration profiles showed a local minimum at the depth of the thermocline (adjacent to a O$_2$ maximum nearby, *see* also Fig. S3), suggesting enhanced respiration at the density gradient (Fig. 2). In August 2017, this feature was also associated with a local turbidity increase at the thermocline (7–8 m, backscatter in Fig. 3B).

Zooplankton, bacteria, and planktonic detritus

The zooplankton population of Lake Cadagno was interchangeably dominated by either cyclopoid and calanoid copepods (i.e., *Cyclops abyssorum tatricus*, *Acanthodiaptomus denticornis*) and their nauplii, or by cladocerans (i.e., *Daphnia longispina*, *Bosmina longirostris*, Fig. 4). In 2016, *Cyclops* were most abundant in July (up to 25 ind. L^{-1}) at

the bottom of the mixolimnion (11 m), but were then gradually replaced by *Daphnia*, which reached high densities (up to 50 ind. L^{-1}) in August, particularly within the thermocline (6–7 m). Overall zooplankton numbers decreased significantly in fall (September). The two most striking features in 2017 were the massive occurrence of *Bosmina* sp. (up to 60 ind. L^{-1}) in the lower mixolimnion in July, and the large increase in the number of nauplii (up to 100 ind. L^{-1}) within the thermocline in August. In general, the zooplankton abundance in summer was almost twice as high in 2017 (8.5 ind. L^{-1}) as in 2016 (5.5 ind. L^{-1}) or in 2018 (4.8 ind. L^{-1}, ANOVA, $p < 0.01$). The zooplankton population in June 2018 was dominated by nauplii (up to 25 ind. L^{-1}). During the dryer months of June/July in 2018, the abundance of zooplankton was lower than during the same period of 2016 and 2017, and the community in the upper water column was numerically dominated by *Daphnia* and calanoid copepods, as well as rotifers in July and by *Daphnia* and nauplii in August. Bacterioplankton in the upper water column (1–10 m) was twice as abundant during summer 2017 as compared to the Summer 2018, with average cell counts between 2.8 and 5.5 × 10^6 cells mL^{-1} and between 1.4 and 2.8 × 10^6 cells mL^{-1} in August and July 2017 and 2018, respectively. Overall, microbial cell counts were higher
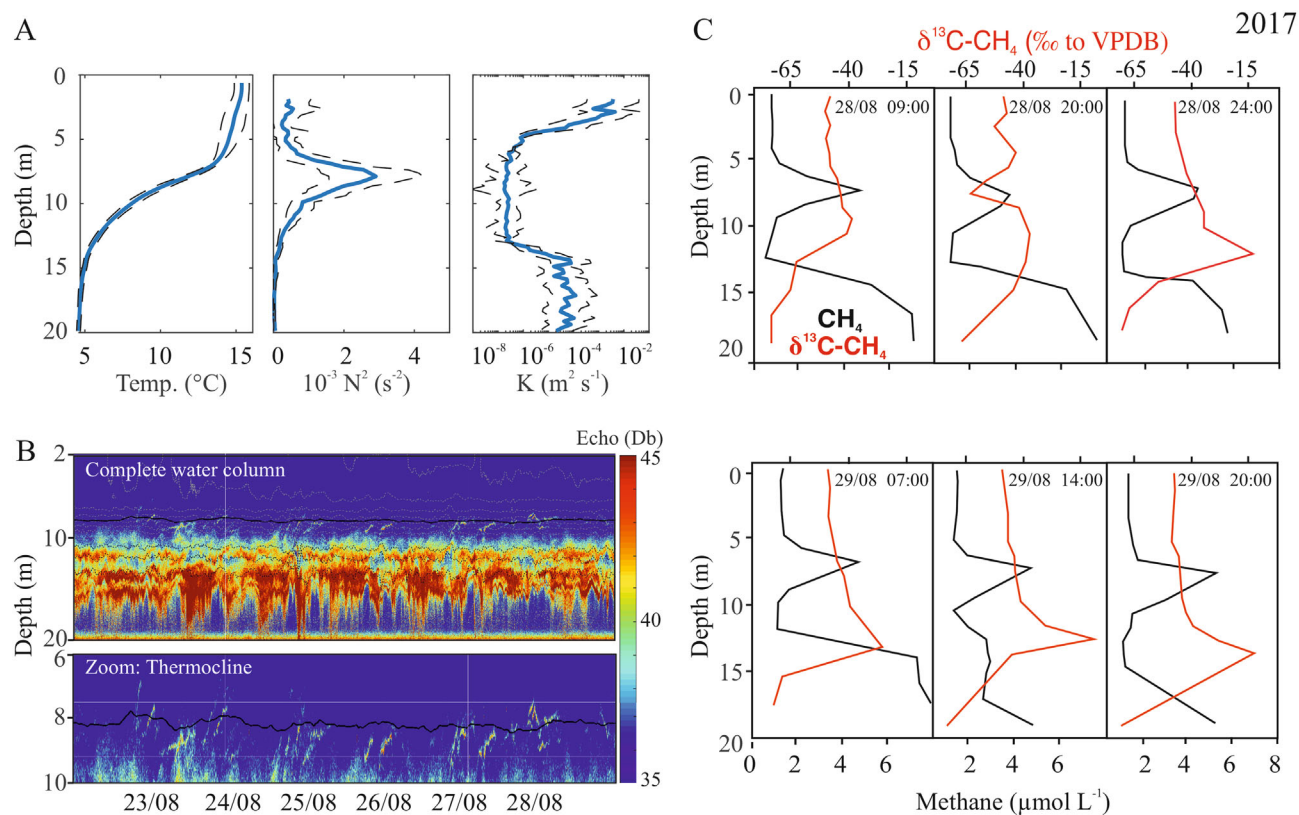
Fig. 3. (**A**) Mean temperatures and buoyancy frequencies—N^2 (in blue with SDs as black dashed lines) as well as diapycnal Osborn–Cox diffusivities—K (Osborn and Cox 1972) as mean for a log-normal distribution (blue line) with its respective intermittency factor (Baker and Gibson 1987; black dashed lines). (**B**) Temporal evolution of echo-sounding from the signature 1000 MHz ADCP showing a relative peak in backscattering in the vicinity of the thermocline (black line). Dashed gray lines represent 1°C isotherms (between 9°C and 17°C). (**C**) Diurnal evolution of CH_4 concentrations and its $\delta^{13}C$ signatures in Lake Cadagno between 28 and 29 August 2017.

within the thermocline and below (down to 10 m) than in surface waters (Fig. 4).

Seasonal changes in the distribution of zooplankton-derived detritus in the upper water column (0–10 m deep) showed a clear and significant correlation to zooplankton abundance (Fig. 4, $R^2 = 0.7$, $F = 45$, $p = 0.0001$). For example, the most pronounced accumulation of zooplankton detritus during summer 2017 was observed at the same depth where also the highest numbers of *Bosmina* sp. and nauplii were present in the water column. At that time, maximum zooplankton detritus concentrations (80 particles L^{-1}) were almost an order of magnitude higher than in 2016 and 2018 (11 and 25 particles L^{-1}, respectively). Analysis of the echo sounding data from the campaign in 2017 revealed peaks of particle concentrations in this water layer (Fig. 3B). The relative magnitude of the observed local maximum was not constant over the day, indicating that the signal is representative for particles aggregating within this density gradient. Given the microscopic observations, such increase in backscattering within the thermocline can be interpreted as accumulation of zooplankton and zooplankton-derived detritus. Whereas our data do not allow for a temporally resolved quantitative

assessment of the relationship between the "strength" of density gradients and the concentration of planktonic detritus, they nevertheless support links between detrital accumulations and stratification in the upper water column.

Spatiotemporal variations in CH_4 concentration and C-isotopic composition

Whenever it was evident (i.e., between July and August), the epilimnetic CH_4 concentration maximum was located within the thermocline. Noticeably, we did not observe any subsurface CH_4 concentration maximum when the surface mixed layer reached depths below 8 m (e.g., September 2016 and 2017, Figs. 2, 4), or during inverse wintertime stratification (manuscript in preparation). The magnitude of CH_4 accumulation within the thermocline varied between the years, with highest peak concentrations in 2017 reaching 6.3 μmol L^{-1} as compared to maximum concentrations of 2.7 μmol L^{-1} in 2018 (Fig. 4; Table 1). There was a significant relationship between CH_4 concentrations in the upper water column and the accumulation of microscopically visible zooplankton detritus ($R^2 = 0.43$, $F = 35$, $p = 0.0001$). Methane concentrations within the epilimnetic maximum were two to
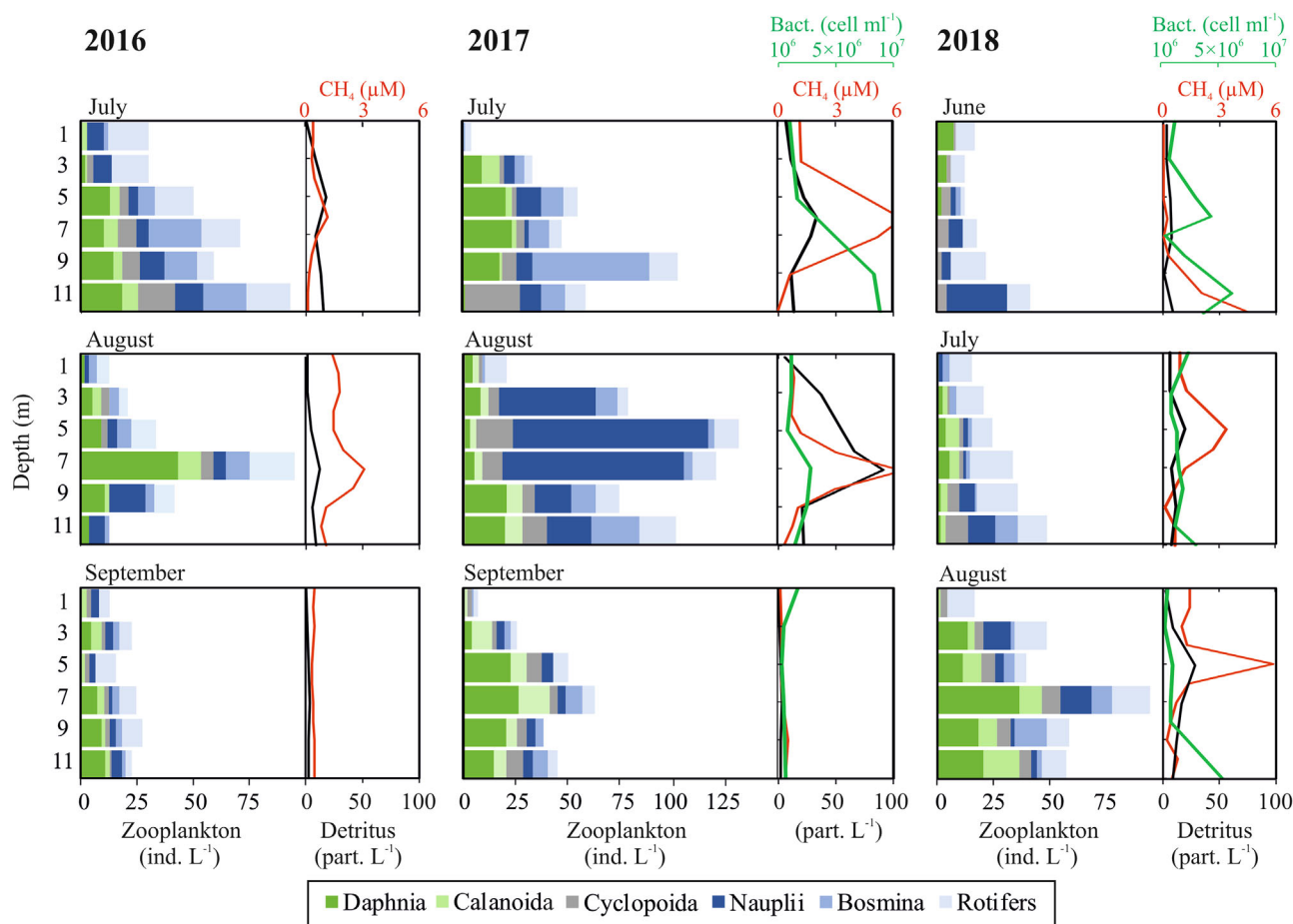
Fig. 4. Interannual and monthly changes in the zooplankton abundance and community structure (bars), as well as associated variability in concentrations of CH_4 (red line), zooplankton detritus (black line) and bacterial numbers (cells/mL in green; for 2017 and 2018 only) in the mixolimnion of Lake Cadagno between July 2016 and August 2018.

six times higher than those in the littoral zone (in 2018 and 2017, respectively) and the total accumulated CH_4 was 5–15 times greater (Table 1). Moreover, the mean $\delta^{13}C$ signature of the pelagic CH_4 at the depth of the concentration peak was distinct (i.e., 41.8 ± 0.5‰) from the $\delta^{13}C$ signature in the epilimnion above (-48.5 ± 4.3‰, $p = 0.01$, $t = 9.5$, $n = 72$) and in the littoral zone of the lake (-52.1 ± 1.1‰, $p = 0.01$, $t = 10.7$, $n = 54$). Very low methanotrophic activity was detected around the CH_4 peak (10 ± 8 nmol d^{-1}), but MOx increased rapidly below 10 m (up to 300 nmol d^{-1}, data not shown) resulting in $\delta^{13}C$ signatures between -12‰ and -30‰. Upward diffusing benthic CH_4 was also different with regards to its $\delta^{13}C$ signature, with $\delta^{13}C$ values of -65‰, thus much lower than observed for the CH_4 in the well oxygenated upper water column. A direct input from the hypolimnetic CH_4 pool (e.g., by ebullition) can thus be excluded.

The diurnal sampling conducted in August 2017 revealed that the lake interior was highly stratified with a stability (N^2) maximum along the thermocline. This high stability region was associated to low dissipation and diffusivity levels

(Fig. 3A). The accumulation of planktonic detritus (two to three times more abundant than in the water layers directly above and below) and the CH_4 accumulation with concentrations between 4.2 and 6.8 μmol L^{-1} (at sundown of 28 and 29 August, respectively) were linked (Fig. 3B,C). Aside from one single $\delta^{13}C$-CH_4 profile taken during sundown of 28 August, when CH_4 within the thermocline was somewhat ^{13}C-depleted (mean of -54‰), we did not observe any significant variability between day and night, neither for CH_4 concentrations nor for the $\delta^{13}C$ signatures.

In order to better constrain the potential generation of the methane paradox through lateral advection of CH_4-containing waters from the littoral zone, we have compared the water isotope signatures (δD and $\delta^{18}O$) between open-lake epilimnetic, thermocline, and littoral waters. While epilimnetic and littoral waters were similar (in terms of their δD signatures, -81.4‰ vs. -80.9‰, $n = 36$, $Q = 0.05$, $p = 0.01$, Table 1), the water within the thermocline (-82.4‰) was different from these water masses ($Q = 2.69$, $p = 0.05$) and from water in the hypolimnion (-86.7‰, $Q = 3.5$, $p = 0.003$). With regards to

Table 1. Concentrations and total amount of CH$_4$ (integrated), as well as ^{13}C-CH$_4$ and D$_2$^{18}O signatures in the epilimnion (0–5 m, offshore), within the thermocline (5–8 m) and in the littoral zone (0–2 m deep inshore) of Lake Cadagno during the summers 2017 and 2018.

	CH$_4$ (µmol L^{-1})	CH$_4$ (mol)	^{13}C (‰)	D$_2$O (‰)	H$_2$^{18}O (‰)	CH$_4$ (µmol L^{-1})	CH$_4$ (mol)	^{13}C (‰)	D$_2$O (‰)	H$_2$^{18}O (‰)
2017		Jul					Aug			
Epilimnion	1.20 (0.1)	42.2 (8)	−47.5 (0.6)	−82.1 (0.3)	−11.6 (0.02)	0.8 (0.04)	29.3 (1)	−47.7 (0.6)	−80.4 (0.15)	−11.0(0.09)
Thermocline	5.3 (0.5)	227.8 (30)	−39.4 (3.7)	−83.6 (1.1)	−12.1 (0.3)	3.4 (2.1)	125.8 (77)	−41.9 (2.1)	−82.6 (0.26)	−11.4 (0.07)
Littoral	0.92 (0.3)	15.2 (5)	−49.3 (0.5)	−81.70 (0.4)	−11.7 (0.1)	0.81 (0.1)	13.4 (1)	−55.2 (0.9)	−80.9 (0.19)	−11.1(0.09)
2018		Jul					Aug			
Epilimnion	1.11 (0.3)	18.4 (5)	−50.4 (0.4)	−82.6 (0.2)	−11.9 (0.1)	1.1 (0.3)	47.8 (13)	−48.8 (0.4)	−82.4 (0.2)	−11.3 (0.07)
Thermocline	2.1 (0.6)	96.0 (30)	−43.6 (6.7)	−84.5 (0.9)	−12.4 (0.1)	2.3 (2.0)	115 (90)	−43.0 (5.1)	−84.1 (0.1)	−11.7 (0.1)
Littoral	1.25 (0.8)	20.6 (12)	−53.2 (2.1)	−82.5 (0.3)	−11.9 (0.2)	0.6 (0.2)	9.3 (3)	−49.8 (0.7)	−81.5 (0.2)	−11.2 (0.1)

SE for each value is shown in parenthesis.

oxygen isotopic signatures, the water-isotopic differentiation was less evident, with only subtle δ^{18}O offsets between water masses from the epilimnion, thermocline and littoral zone (−11.1‰, −11.6‰, and −11.46‰, respectively) and water in the hypolimnion (−12.1‰, $n = 36$, $Q > 3.7$, $p < 0.001$).

In vitro CH$_4$ production by zooplankton and associated detritus

While CH$_4$ concentration changes in incubations with cladocerans were indistinguishable from the control (Fig. 5B, ANOVA, $p = 0.9$), incubation of adult copepods and their nauplii resulted in an increase of CH$_4$ that, by the end of the experiments, were significantly higher than in the control (Fig. 5A; $p = 0.01$, $F = 6$). The rate of increase in CH$_4$ was largest for incubations with molting nauplii. Incubation of concentrated plankton-derived detritus revealed consistent CH$_4$ production under fully oxygenated conditions, with CH$_4$ concentrations reaching up to 15.5 ± 0.2 nmol L^{-1} (Fig. 5C). The amount of CH$_4$ produced was correlated ($R^2 = 0.85$, $F = 40$, $p = 0.004$) to the concentration of detritus, with the lowest (0.56 nmol L^{-1} CH$_4$ d^{-1}) and highest (0.8 nmol L^{-1} CH$_4$ d^{-1}) production rates in the treatments with the lowest and highest detritus concentrations, respectively. However, the relationship was not directly proportional. Normalized for biomass, CH$_4$ production during oxic incubations decreased with increasing detritus concentration, showing rates between 0.095 and 0.046 nmol L^{-1} CH$_4$ mg dry mass L^{-1} d^{-1} for low and high amounts of incubated detritus, respectively. Methane formation in zooplankton-detritus under oxic conditions was enhanced by up to 10 times upon amendment with MPn. Direct CH$_4$ production from the added MPn, most likely through exploitation by natural consortia of microbes associated to the zooplankton detritus, was confirmed by ^{13}C-CH$_4$ fingerprinting. That is, with the accumulation of CH$_4$, its δ^{13}C approximated the δ^{13}C signature of the added MPn (δ^{13}C of $−101 \pm 0.5$‰; squares in Fig. 5D) indicating de-methylation of the MPn to form CH$_4$ (Taenzer et al. 2020).

Zooplankton-associated microbiome

The microbial community structures in the three size fractions (0.2–2.7, 2.7–20, > 20 µm) was different (PERMANOVA, $F = 2.1$, $R^2 = 0.58$, $p = 0.07$) with the highest diversity found in the largest size class (Fig. S4A,B). The community change induced by the addition of MPn, however, was not significant (PERMANOVA, $F = 0.68$, $R^2 = 0.14$, $p = 0.7$). The analysis of the microbiome associated to large plankton detritus (fraction > 20 µm) accumulating within the thermocline of Lake Cadagno revealed the dominance of Proteobacteria (47%) and other bacteria that belonged to the Bacteroidetes (18%) and the Verrucomicrobia (9%) phyla. The 25 most abundant taxa represented 69.7% of the total community and included, for example, *Sphingobium* (7.3%, *Alphaproteobacteria*), *Azospirillum* (6.8%, Alphaproteobacteria) and *Flavobacterium* (4.8%, Bacteroidetes), as well as *Prosthecobacter* (4%,

Verrucomicrobia) and *Emticicia* (3.7%, Bacteroidetes; Table S1). Upon addition of MPn, five new taxa emerged among the 25 most abundant taxa. These included *Acinetobacter*, *Polaromonas*, *Sandarakinorhabus*, *Rhodovarius*, and *Novosphingobium*. Among common groups, the relative abundance of *Prosthecobacter* and *Reyranella* increased most upon MPn addition (Table S1). The relative abundance of methanogenetic Archaea was very low (i.e., < 0.05%). In the whole dataset, only 45 OTUs were identified as Archaea (of 1554 in total), and among those, only four OTUs represent common methanogens belonging to the Methanomicrobiales (*Methanoregula* sp.: OTU174, OTU256) and the Methanomassilicoccales (OTU581, OTU611, File S2). Quantitative PCR of the mcrA gene (i.e., indicative of methanogenic Archaea) resulted in primer dimers and unspecific products during late amplification cycles because of the low abundance of the target gene. Subsequent agarose gel electrophoresis confirmed the presence of mcrA only in two of the samples: "Cad_Aug18_7m_Non_ > 2.7" and "Cad_Aug18_Contr_Zoopl" with 101 and 65 mcrA gene copies per ng^{-1} extracted DNA, respectively (Table S2). The absent/low copy numbers and the fact that there was no significant difference between experimental treatments (+MPn/−MPn), further support that classic methanogen associated to the concentrated zooplankton detritus did not control the observed patterns of CH_4 accumulation.

Discussion

Potential sources of methane in oxygenated waters and biophysical controls

Previous work showed that the methane paradox in lakes can be sustained through the lateral transport of CH_4-rich waters from the littoral zones (Peeters et al. 2019), where CH_4 is produced through canonical (i.e., anaerobic) methanogenesis in the sediments. While our observations do not unequivocally preclude the contribution of lateral transport to the formation of the methane paradox in Lake Cadagno, they support an alternative mechanism related to in situ production. First, our CH_4 budget considerations (Table 1) implies increasing CH_4 accumulation along the littoral-pelagic continuum, in contrast to what would be expected if the (highly productive) littoral sediments were the primary source of the pelagic CH_4 peak (Encinas Fernández et al. 2016). Second, the isotopic signatures (i.e., δD-H_2O and $δ^{13}C$-CH_4) for the water masses in the littoral zone vs. the epilimnion are sufficiently distinct to conclude that lateral transport of inshore CH_4 could not fully sustain the offshore CH_4 accumulations. Similarly, the $δ^{13}C$ signature of the CH_4 in the thermocline was distinct from the $δ^{13}C$ signature of the upward diffusing CH_4 produced in the sediments and anoxic hypolimnion, so that direct CH_4 transport from bottom waters can also be excluded.

Arguing that the observed epilimnetic CH_4 concentration peak results from in situ aerobic CH_4 production, we attempt to further constrain the potential pelagic CH_4 sources. In contrast to recent findings, our field results do not provide direct support for the strong influence of light dependent CH_4 formation (either biotic or abiotic, i.e., Zhou et al. 2018; Bižić et al. 2020). That is, during the diurnal sampling, we did not observe differences between daytime and nighttime CH_4 concentrations. However, considering previous field and laboratory efforts, which provide evidence that links between photosynthetic activity by phytoplankton and methane production exist, more work (e.g., on the isotopic signatures of photosynthetically produced CH_4) is needed to better constrain the role of phytoplankton regarding the CH_4 paradox in Lake Cadagno. The incubations of active zooplankton also did not provide evidence for a consistent methane release in feeding animals, and production was much lower than what was observed during incubations of copepods from the Baltic Sea (Schmale et al. 2018). A more consistent CH_4 release was observed in incubations with concentrated zooplankton detritus (Fig. 5C) further supporting our field observations, which indicated the link between CH_4 concentrations and the accumulation of detritus. The calculated CH_4 production rates during detritus incubations were low (up to 1 nmol L^{-1} d^{-1}) when compared to recent estimates of aerobic CH_4 production required to sustain the paradox in other lakes (i.e., 19–200 nmol L^{-1} d^{-1}; Bogard et al. 2014; Günthel et al. 2019), but were in the range of results from the most recent incubations of marine zooplankton (i.e., Stawiarski et al. 2019). Considering the measured range of MOx rates within the thermocline of Lake Cadagno during the summer (0–50 nmol d^{-1}), assuming quasi-steady state, and excluding any lateral inflows, CH_4 production rates of at least 10–20 nmol L^{-1} d^{-1} would be needed to sustain the observed methane paradox. However, CH_4 formation (or the methane-producing potential) in our incubations was possibly affected by the preprocessing of lake water and zooplankton detritus.

The correspondence between the CH_4 concentration peak and the region of plankton detritus accumulation with the depth of the strong water-density gradient implies that water-column stratification plays an important role with regards to concentrating organic particles and oxic production of CH_4. Putative links etween the methane paradox and the retention of OM along density gradients is likely not limited to detritus but may also involve allochthonous OM, which likely hold a similar potential to fuel CH_4 production (either directly as methanogenetic substrates, or indirectly through stimulating plankton biomass). In this regard, both the meteorological conditions that control density stratification, as well as the interactions that govern the inputs of OM may modulate the methane paradox, explaining part of the observed variability in CH_4 accumulation. Notwithstanding the potential contribution from allochthonous OM in the formation of the methane paradox, our pelagic vs. littoral CH_4 budgets, the isotopic
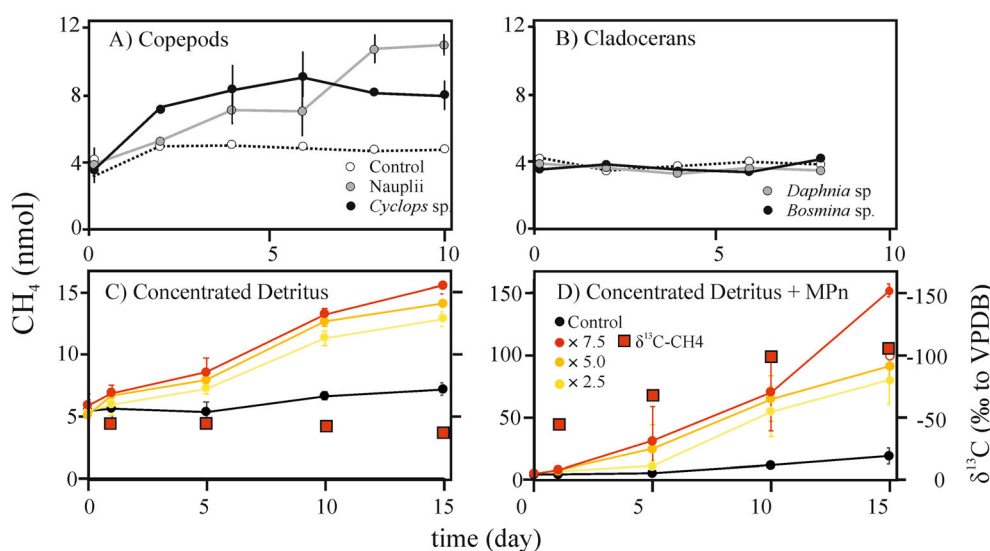
Fig. 5. Evolution of the dissolved CH_4 during incubation of: (**A**) copepods and (**B**) cladocerans. (**C**) Methane production from concentrated zooplankton detritus (2.5, 5.0, and 7.5 times with respect to control) and (**D**) from concentrated zooplankton detritus amended with ^{13}C-labeled MPn. Note the different axis scales. ^{13}C-CH_4 is illustrated by red squares in panels **C** and **D**.

constraints, and additional results from a winter sampling of the ice-covered Lake Cadagno (in preparation) all argue against lateral transport being responsible for direct "injection" of methane-rich littoral waters into the epilimnion.

Indirect relationship between seasonal lateral inflows and aerobic CH_4 formation may explain some variability of the methane paradox in lakes (DelSontro et al. 2018b). For instance, higher precipitation rates in the catchment of Lake Cadagno in 2017 may have increased the import of terrestrial OM to the lake (similar effects described by Solomon et al. 2015). While we did not investigate allochthonous OM fluxes, nor their potentially stimulating effect on plankton, the correspondence between the high precipitation (2017) on the one hand, increased plankton production (*see* also Tanentzap et al. 2017; Adamczuk et al. 2019), microbial biomass and CH_4 accumulation on the other (Fig. 4), implies that the methane paradox is, to some extent, moderated by allochthonous inputs (modulated through changeable weather patterns; Schindler et al. 1996; Parker et al. 2008).

Pathways of zooplankton-associated methane formation

While incubations of active zooplankton did not result in consistent CH_4 release, we observed a more systematic CH_4 production in incubations with zooplankton detritus. This observation supports a passive rather than an active role (i.e., methane production during feeding) of zooplankton in the formation of the lacustrine methane paradox. More importantly, methane production rates increased with the amount of zooplankton detritus (although not in a 1 : 1 proportional fashion), attesting to the direct involvement of the detritus in this process. Based on the molecular evidence (*see* below), we argue that the observed CH_4 production was

mostly independent of canonical methanogenesis by *Archaea* using low-molecular weight carbon substrates typically derived during fermentative processes in the O_2-free microniches (i.e., acetate). In the same vein, the fact that the CH_4 generation was not directly (i.e., 1 : 1) proportional to the amount of incubated biomass supports that observable CH_4 production was, at least partly, associated to the bacterial exploitation of nonclassical substrates that became more available during progressing zooplankton biomass decomposition (i.e., methylated polysaccharides or methylamines; Repeta et al. 2016; Wang et al. 2021, but *see* Fig. S5).

Noncanonical, aerobic methane formation could be related to the degradation of dissolved organic compounds, such as methylated dissolved organic phosphorus (DOP) compounds (Karl et al. 2008; Repeta et al. 2016). While the origin of MPn in freshwaters is still uncertain, its degradation contributes to the formation of methane paradox in the ocean (Karl et al. 2008). Our oxic phosphonate-amended incubations support that the microbiome associated to zooplankton-detritus (Fig. S1) is capable to quantitatively produce CH_4 from MPn. While we have used MPn concentrations (i.e., 200 nmol L^{-1}) that are likely higher than those found in natural freshwaters (i.e., up to 20 nmol L^{-1}, Whitney and Lomas 2019), exploitation of other methylated DOP compounds (i.e., polysaccharide esters of phosphonic acids, Repeta et al. 2016) or methylamines (Wang et al. 2021) follows a similar pathway and can thus liberate CH_4 to oxic waters.

Recent work provides ample evidence for the importance of DOP, including phosphonates, in freshwaters and in the ocean (Whitney and Lomas 2019). Similarly, ongoing analysis of DOM from Lake Cadagno using Fourier-transform mass spectrometry combined with nuclear magnetic resonance indicates

that methylated DOP in oxic lake waters contributes as much as 25% to the total DOP pool (unpublished data). Particularly under severe inorganic P-depletion (i.e., summertime in Lake Cadagno), CH_4 is efficiently generated during methylated-DOP exploitation (Yao et al. 2016). However, inorganic P scarcity is not necessarily a precondition, as CH_4 formation from methylated phosphonates may also occur when ambient levels of inorganic P (DIP) are relatively high (Fox and Mendz 2006). Indeed, analyses from our incubations revealed that, upon the introduction of concentrated zooplankton detritus, DIP concentrations reached up to 20 ± 6 μmol L^{-1} (as PO_4^{3-}) within the first 24 hours of incubation. Despite the replete-DIP conditions, CH_4 was still produced, and its distinct $\delta^{13}C$ signature shows that it was generated from the MPn (Taenzer et al. 2020).

The zooplankton detritus-associated microbiome was responsive to the addition of MPn. Yet, interestingly, the relative abundance of methanogenic *Archae*a was low (i.e., < 0.05%) in all incubations, and mcrA remained undetectable in all incubations with added MPn, again implying that the observed methane production was related to bacterial rather than archaeal metabolism of methylphosphonates. While the ability to exploit phosphonates as a P source is widespread throughout aquatic ecosystems and microbiomes, several different phosphonate-utilization mechanisms have been described (i.e., McGrath et al. 1995; Kononova and Nesmeyanova 2002; Martinez et al. 2010; Gomez-Garcia et al. 2011). Regardless, however, of the exact mechanism involved in the cleavage of C to P bonds (*see* Sosa et al. 2019), the transport mechanism of phosphonates, involving phosphonate-binding-proteins (PhnD), is shared across all microbial phyla capable of metabolizing MPn. Indeed, the gene encoding PhnD is found in numerous marine bacterial genomes, including those of globally widespread marine bacteria (i.e., *Trichodesmium*; Dyhrman et al. 2006), *Synechococcus*, *Prochlorococcus*, and *Pelagibacter* (Feingersch et al. 2012). The presence of phnD in the water column was also confirmed for Lake Cadagno, with the highest relative abundance of this gene found at the thermocline during summer (Venetz 2019). Moreover, bacteria enriched during our MPn-amended incubations included many taxa that have been evidenced to contain this phosphonate-utilization marker gene (i.e., *Acinetobacter* sp., *Shingobium*). Hence, it is reasonable to assume that at least part of the observed methane production along the thermocline of Lake Cadagno is related to the metabolism of methylated DOP (i.e., MPn) by detritus-associated microbes, and that seasonal and interannual variation in CH_4 accumulation are likely tied to the dynamics of both detritus accumulation and bacterial community structure.

During the experiment, the microbial community change was associated with an increase in cell abundance by a factor of two during incubations with MPn, as compared to the unamended control. Similarly, in the Lake Cadagno water column, microbial cell numbers within the thermocline also increase together with the abundance of zooplankton and

planktonic detritus (Figs. 3, 4). Our combined field and experimental results further support the hypothesis that detritus aggregating along density gradients provides a biogeochemical hotspot for heterotrophic bacteria (Grossart and Simon 1993; MacIntyre et al. 1995; Bižić-Ionescu et al. 2018) and, potentially, methylated-DOP exploitation. While we cannot resolve the source of methylated-DOP compounds, we argue that they are abundant enough to potentially serve as a significant lake-wide source of P and CH_4. Ongoing quantitative work on the molecular characterization of DOM (at in situ concentrations of 0.6–2.0 mgC L^{-1}) and methylated DOP in Lake Cadagno together with experimental incubations (i.e., rate measurements) will help to establish whether de-methylation of these compounds may generate enough CH_4 to explain the observed accumulation.

Zooplankton community structure and aerobic methane formation

As elaborated above, we assign a more important role to zooplanktonic detritus rather than to active zooplankton itself with regards to aerobic methane production. Yet, quite obviously, the two are intrinsically linked. In Lake Cadagno, formation and magnitude of the methane paradox was correlated to both the abundance of zooplankton and the amount of zooplankton-related detritus. Abundance of zooplankton, its behavior and resulting detritus, in turn, depend on the distribution of food (Gulati and DeMott 1997) and, thus, on bacterial and phytoplankton production.

Previous work demonstrated that the higher primary productivity and warming enhance benthic methanogenesis, supporting the link between lake trophic status and CH_4 emissions (e.g., Bartosiewicz et al. 2015, 2016; Davidson et al. 2015, 2018). Our results add a novel twist to productivity-CH_4 coupling in lakes by showing that rates of oxic methane formation may depend directly on heterotrophic production. Factors affecting zooplankton in the epilimnion, such as temperature, food, predation (Marino et al. 2020), and thermocline depth (Sastri et al. 2014) can, in turn, affect the rates of oxic CH_4 production. Consequently, the interaction between the hydrodynamic conditions and zooplankton community characteristics may be regarded as potential driver of temporal changes in the occurrence and magnitude of the lacustrine methane paradox, and its role in regulating CH_4 efflux from lakes to the atmosphere.

The link between zooplankton community, detritus, and the methane paradox in Lake Cadagno was most obvious during the rainy summer of 2017, when the highest concentrations of CH_4 were measured along with high amounts of detritus originating from *Bosmina* sp. and nauplii (Fig. 4 and microscopic evaluation). In our incubations, CH_4 was also produced mostly from the detritus of cyclopoid copepods and their nauplii, as large cladocerans were absent during water collection for these experiments (in June 2018). We argue that food web processes stimulating blooms of zooplankton may

favor consecutive CH_4 formation from species-specific detritus. In this context, it is important to underline that, while the guts of large cladocerans are considered fully aerobic (e.g., Freese and Schink 2011), the guts of cyclopoid copepods and small cladocerans are inhabited by a whole spectrum of both aerobic and anaerobic microbes (e.g., Tang et al. 2006). Based on the molecular data in hand, we argue that classic methanogenesis in anoxic micro-niches (i.e., including anoxic guts of zooplankton) per se does not play an important role during the formation of the methane paradox in Lake Cadagno. Yet, a more complex microbiome originating from diverse intestinal habitats will unequivocally widen the metabolic spectrum of usable methylated substrates (Bandh et al. 2019; Wäge et al. 2019). This, in turn, will increase the probability of CH_4 formation from planktonic detritus and various noncanonical substrates.

Conclusion

Our results highlight the importance of detritus-hosted methanogenesis in the CH_4 budget of oxic freshwaters. The observed temporal variability in subsurface CH_4 concentrations underlines the need for better understanding of direct and indirect factors that modulate the magnitude of the freshwater methane paradox. We demonstrate that changes in zooplankton phenology and hydrodynamic conditions, by influencing rates of plankton-detritus accumulation and its retention along density gradients, affect the magnitude of CH_4 accumulation in oxic waters. This effect operates, most likely, through acquisition and degradation of methylated organics by the detritus-associated microbiome. Based on our observational constraints on the methane paradox in Lake Cadagno and experimental data, we argue that for improved predictions of lacustrine methane production and related emission an in-depth understanding of the interlinkages between hydrodynamic conditions and plankton community structure is needed. Accumulation of CH_4 in oxygenated pelagic waters results from a complex interplay between physical and biogeochemical processes, and the relative contribution is likely to be lake-specific.

Future strengthening of the stratification in global lakes, and the associated enhancement of density discontinuities, can be anticipated to decrease the sinking rates of organic detritus and result in greater retention of aggregated particles and their microbiome in oxygenated waters. Enhanced production and accumulation of detritus-derived CH_4 in the oxic waters of warmer and potentially more strongly stratified lakes will in turn lead to higher efflux of this potent GHG to the atmosphere.

Data availability statement

The biogeochemical datasets generated during and/or analyzed during the current study are available from the corresponding author upon request. All microstructure data is archived in the OA repository at: https://doi.org/10.5281/zenodo.3507638. The raw sequences have been deposited at NCBI under the Bioproject number PRJNA743306 (Accessions: SAMN20009058–SAMN20009063).

References

Adamczuk, M., B. Ferencz, T. Mieczan, and J. Dawidek. 2019. Allochthonous subsidies as driving forces for development of plankton in an autotrophic, temperate, and small lake. Hydrobiologia **846**: 59–73. doi:10.1007/s10750-019-04052-9

Ambler, J. W. 2002. Zooplankton swarms: Characteristics, proximal cues and proposed advantages. Hydrobiologia **480**: 155–164. doi:10.1023/A:1021201605329

Baker, M. A., and C. H. Gibson. 1987. Sampling turbulence in the stratified ocean: Statistical consequences of strong intermittency. J. Phys. Oceanogr. **17**: 1817–1836. doi:10.1175/1520-0485(1987)017<1817:STITSO>2.0.CO;2

Bandh, S. A., S. Shafi, N. Shameem, R. Dar, A. N. Kamili, and B. A. Ganai. 2019. Spatio-temporal patterns of bacterial diversity along environmental gradients and bacterial attachment to organic aggregates, p. 137–174. *In* S. A. Bandh, S. Shafi, and N. Shameem [eds.], Freshwater microbiology. Academic Press.

Bartosiewicz, M., I. Laurion, and S. MacIntyre. 2015. Greenhouse gas emission and storage in a small shallow lake. Hydrobiologia **757**: 101–115. doi:10.1007/s10750-015-2240-2

Bartosiewicz, M., I. Laurion, F. Clayer, and R. Maranger. 2016. Heat-wave effects on oxygen, nutrients, and phytoplankton can alter global warming potential of gases emitted from a small shallow lake. Environ. Sci. Technol. **50**: 6267–6275.

Bartosiewicz, M., A. Przytulska, J. F. Lapierre, I. Laurion, M. F. Lehmann, and R. Maranger. 2019. Hot tops, cold bottoms: Synergistic climate warming and shielding effects increase carbon burial in lakes. Limnol. Oceanogr.: Lett. **4**: 132–144. doi:10.1002/lol2.10117

Bižić, M., T. Klintzsch, D. Ionescu, M. Y. Hindiyeh, M. Günthel, A. M. Muro-Pastor, and H. P. Grossart. 2020. Aquatic and terrestrial cyanobacteria produce methane. Sci. Adv. **6**: eaax5343. doi:10.1126/sciadv.aax5343

Bižić-Ionescu, M., D. Ionescu, and H. P. Grossart. 2018. Organic particles: Heterogeneous hubs for microbial interactions in aquatic ecosystems. Front. Microbiol. **9**: 2569. doi:10.3389/fmicb.2018.02569

Bogard, M. J., P. A. Del Giorgio, L. Boutet, M. C. G. Chaves, Y. T. Prairie, A. Merante, and A. M. Derry. 2014. Oxic water column methanogenesis as a major component of aquatic CH_4 fluxes. Nat. Commun. **5**: 5350. doi:10.1038/ncomms6350

Davidson, T. A., J. Audet, J. C. Svenning, T. L. Lauridsen, M. Søndergaard, F. Landkildehus, and E. Jeppesen. 2015. Eutrophication effects on greenhouse gas fluxes from

shallow-lake mesocosms override those of climate warming. Glob. Chang. Biol. **21**: 4449–4463. doi:10.1111/gcb.13062

Davidson, T. A., J. Audet, E. Jeppesen, F. Landkildehus, T. L. Lauridsen, M. Søndergaard, and J. Syväranta. 2018. Synergy between nutrients and warming enhances methane ebullition from experimental lakes. Nat. Clim. Change **8**: 156–160. doi:10.1038/s41558-017-0063-z

de Angelis, M. A., and C. Lee. 1994. Methane production during zooplankton grazing on marine phytoplankton. Limnol. Oceanogr. **39**: 1298–1308. doi:10.4319/lo.1994.39.6.1298

Del Don, C., K. W. Hanselmann, R. Peduzzi, and R. Bachofen. 2001. The meromictic alpine Lake Cadagno: Orographical and biogeochemical description. Aquat. Sci. **63**: 70–90. doi:10.1007/PL00001345

DelSontro, T., J. J. Beaulieu, and J. A. Downing. 2018*a*. Greenhouse gas emissions from lakes and impoundments: Upscaling in the face of global change. Limnol. Oceanogr.: Lett. **3**: 64–75. doi:10.1002/lol2.10073

DelSontro, T., P. A. del Giorgio, and Y. T. Prairie. 2018*b*. No longer a paradox: The interaction between physical transport and biological processes explains the spatial distribution of surface water methane within and across lakes. Ecosystems **21**: 1073–1087. doi:10.1007/s10021-017-0205-1

Dyhrman, S. T., P. D. Chappell, S. T. Haley, J. W. Moffett, E. D. Orchard, J. B. Waterbury, and E. A. Webb. 2006. Phosphonate utilization by the globally important marine diazotroph *Trichodesmium*. Nature **439**: 68–71. doi:10.1038/nature04203

Edgar, R. C. 2013. UPARSE: highly accurate OTU sequences from microbial amplicon reads. Nat. Methods **10**: 996–998. doi:10.1038/nmeth.2604

Edgar, R. C. 2016. SINTAX: a simple non-Bayesian taxonomy classifier for 16S and ITS sequences. bioRxiv. doi:10.1101/074161

Elliott, D. T., and K. W. Tang. 2009. Simple staining method for differentiating live and dead marine zooplankton in field samples. Limnol. Oceanogr.: Methods **7**: 585–594. doi:10.4319/lom.2009.7.585

Encinas Fernández, J., F. Peeters, and H. Hofmann. 2016. On the methane paradox: Transport from shallow water zones rather than in situ methanogenesis is the major source of CH_4 in the open surface water of lakes. J. Geophys. Res.: Biogeo. **121**: 2717–2726. doi:10.1002/2016JG003586

Falcioni, T., S. Papa, and J. M. Gasol. 2008. Evaluating the flow-cytometric nucleic acid double-staining protocol in realistic situations of planktonic bacterial death. Appl. Environ. Microbiol. **74**: 1767–1779. doi:10.1128/AEM.01668-07

Feingersch, R., A. Philosof, T. Mejuch, F. Glaser, O. Alalouf, Y. Shoham, and O. Béja. 2012. Potential for phosphite and phosphonate utilization by *Prochlorococcus*. ISME J. **6**: 827–834. doi:10.1038/ismej.2011.149

Ferry, J. G. 2012. Methanogenesis: Ecology, physiology, biochemistry & genetics. Springer Science & Business Media.

Fox, E. M., and G. L. Mendz. 2006. Phosphonate degradation in microorganisms. Enzyme Microb. Technol. **40**: 145–150. doi:10.1016/j.enzmictec.2005.10.047

Freese, H. M., and B. Schink. 2011. Composition and stability of the microbial community inside the digestive tract of the aquatic crustacean *Daphnia magna*. Microb. Ecol. **62**: 882–894. doi:10.1007/s00248-011-9886-8

Glud, R. N., H. P. Grossart, M. Larsen, K. W. Tang, K. E. Arendt, S. Rysgaard, and T. Gissel Nielsen. 2015. Copepod carcasses as microbial hot spots for pelagic denitrification. Limnol. Oceanogr. **60**: 2026–2036. doi:10.1002/lno.10149

Gomez-Garcia, M. R., M. Davison, M. Blain-Hartnung, A. R. Grossman, and D. Bhaya. 2011. Alternative pathways for phosphonate metabolism in thermophilic cyanobacteria from microbial mats. ISME J. **5**: 141–149. doi:10.1038/ismej.2010.96

Grossart, H. P., and M. Simon. 1993. Limnetic macroscopic organic aggregates (lake snow): Occurrence, characteristics, and microbial dynamics in Lake Constance. Limnol. Oceanogr. **38**: 532–546. doi:10.4319/lo.1993.38.3.0532

Grossart, H. P., K. Frindte, C. Dziallas, W. Eckert, and K. W. Tang. 2011. Microbial methane production in oxygenated water column of an oligotrophic lake. Proc. Natl. Acad. Sci. USA **108**: 19657–19661. doi:10.1073/pnas.1110716108

Gulati, R., and W. DeMott. 1997. The role of food quality for zooplankton: Remarks on the state-of-the-art, perspectives and priorities. Freshw. Biol. **38**: 753–768. doi:10.1046/j.1365-2427.1997.00275.x

Günthel, M., D. Donis, G. Kirillin, D. Ionescu, M. Bizic, D. F. McGinnis, and K. W. Tang. 2019. Contribution of oxic methane production to surface methane emission in lakes and its global importance. Nat. Commun. **10**: 5497. doi:10.1038/s41467-019-13320-0

Karl, D. M., L. Beversdorf, K. M. Björkman, M. J. Church, A. Martinez, and E. F. Delong. 2008. Aerobic production of methane in the sea. Nat. Geosci. **1**: 473–478. doi:10.1038/ngeo234

Karl, D. M., and B. D. Tilbrook. 1994. Production and transport of methane in oceanic particulate organic matter. Nature **368**: 732–734.

Kirillin, G., H. P. Grossart, and K. W. Tang. 2012. Modeling sinking rate of zooplankton carcasses: Effects of stratification and mixing. Limnol. Oceanogr. **57**: 881–894. doi:10.4319/lo.2012.57.3.0881

Kirschke, S., and others. 2013. Three decades of global methane sources and sinks. Nat. Geosci. **6**: 813–823. doi:10.1038/ngeo1955

Kononova, S. V., and M. A. Nesmeyanova. 2002. Phosphonates and their degradation by microorganisms. Biochemistry **67**: 184–195. doi:10.1023/a:1014409929875

Leech, D. M., A. I. Pollard, S. G. Labou, and S. E. Hampton. 2018. Fewer blue lakes and more murky lakes across the continental US: Implications for planktonic food webs. Limnol. Oceanogr. **63**: 2661–2680. doi:10.1002/lno.10967

Lever, M. A., and A. P. Teske. 2015. Diversity of methane-cycling archaea in hydrothermal sediment investigated by general and group-specific PCR primers. Applied and environmental microbiology **81**: 1426–1441. doi:10.1128/AEM.03588-14

MacIntyre, S., A. L. Alldredge, and C. C. Gotschalk. 1995. Accumulation of marines now at density discontinuities in the water column. Limnol. Oceanogr. **40**: 449–468. doi:10.4319/lo.1995.40.3.0449

Martinez, A., G. W. Tyson, and E. F. DeLong. 2010. Widespread known and novel phosphonate utilization pathways in marine bacteria revealed by functional screening and metagenomic analyses. Environ. Microbiol. **12**: 222–238. doi:10.1111/j.1462-2920.2009.02062.x

Marino, J. A., Jr., H. A. Vanderploeg, S. A. Pothoven, A. K. Elgin, and S. D. Peacor. 2020. Long-term survey data reveal large predator and temperature effects on population growth of multiple zooplankton species. Limnol. Oceanogr. **65**: 694–706. doi:10.1002/lno.11340

McGinnis, D. F., J. Greinert, Y. Artemov, S. E. Beaubien, and A. N. D. A. Wüest. 2006. Fate of rising methane bubbles in stratified waters: How much methane reaches the atmosphere? J. Geophys. Res. **111**: C09007. doi:10.1029/2005JC003183

McMurdie, P. J., and S. Holmes. 2013. phyloseq: an R package for reproducible interactive analysis and graphics of microbiome census data. PloS One **8**: e61217. doi:10.1371/journal.pone.0061217

McGrath, J. W., G. B. Wisdom, G. McMullan, M. J. Larkin, and J. P. Quinn. 1995. The purification and properties of phosphonoacetate hydrolase, a novel carbon-phosphorus bond-cleavage enzyme from *Pseudomonas fluorescens* 23F. Eur. J. Biochem. **234**: 225–230. doi:10.1111/j.1432-1033.1995.225_c.x

Milucka, J., M. Kirf, L. Lu, A. Krupke, P. Lam, S. Littmann, and C. J. Schubert. 2015. Methane oxidation coupled to oxygenic photosynthesis in anoxic waters. ISME J. **9**: 1991–2002. doi:10.1038/ismej.2015.12

Oksanen, J., and others. (2020). Vegan: Community ecology package. R Package Version. 2.5-7. CRAN. Available from https://cran.r-project.org

Osborn, T. R., and C. S. Cox. 1972. Oceanic fine structure. Geophys. Fluid Dyn. **3**: 321–345. doi:10.1080/03091927208236085

Oremland, R. S. 1979. Methanogenic activity in plankton samples and fish intestines A mechanism for in situ methanogenesis in oceanic surface waters. Limnol. Oceanogr. **24**: 1136–1141. doi:10.4319/lo.1979.24.6.1136

Orenstein, E. C., D. Ratelle, C. Briseño-Avena, M. L. Carter, P. J. Franks, J. S. Jaffe, and P. L. Roberts. 2020. The Scripps Plankton Camera system: A framework and platform for in situ microscopy. Limnol. Oceanogr.: Methods **18**: 681–695. doi:10.1002/lom3.10394

Parker, B. R., R. D. Vinebrooke, and D. W. Schindler. 2008. Recent climate extremes alter alpine lake ecosystems. Proc. Natl. Acad. Sci. USA **105**: 12927–12931. doi:10.1073/pnas.0806481105

Parada, A. E., D. M. Needham, and J. A. Fuhrman. 2016. Every base matters: assessing small subunit rRNA primers for marine microbiomes with mock communities, time series and global field samples. Environ. Microbiol. **18**: 1403–1414. doi:10.1111/1462-2920.13023

Peeters, F., J. Encinas Fernandez, and H. Hofmann. 2019. Sediment fluxes rather than oxic methanogenesis explain diffusive CH_4 emissions from lakes and reservoirs. Sci. Rep. **9**: 243. doi:10.1038/s41598-018-36530-w

Quast, C., E. Pruesse, P. Yilmaz, J. Gerken, T. Schweer, P. Yarza, J. Peplies, and F. O. Glöckner. 2013. The SILVA ribosomal RNA gene database project: improved data processing and web-based tools. Nucleic Acids Res. **41**: D590–D596. doi:10.1093/nar/gks1219

Reeburgh, W. S., B. B. Ward, S. C. Whalen, K. A. Sandbeck, K. A. Kilpatrickt, and L. J. Kerkhof. 1991. Black Sea methane geochemistry. Deep-Sea Res. Part A Oceanogr. Res. Pap. **38**: S1189–S1210. doi:10.1016/S0198-0149(10)80030-5

Repeta, D. J., S. Ferrón, O. A. Sosa, C. G. Johnson, L. D. Repeta, M. Acker, and D. M. Karl. 2016. Marine methane paradox explained by bacterial degradation of dissolved organic matter. Nat. Geosci. **9**: 884–887. doi:10.1038/ngeo2837

Sampei, M., I. Sasaki, H. Hattori, A. Forest, and L. Fortiera. 2009. Significant contribution of passively sinking copepods to downward export flux in Arctic waters. Limnol. Oceanogr. **54**: 1894–1900. doi:10.4319/lo.2009.54.6.1894

Sasakawa, M., U. Tsunogai, S. Kameyama, F. Nakagawa, Y. Nojiri, and A. Tsuda. 2008. Carbon isotopic characterization for the origin of excess methane in subsurface seawater. J. Geophys. Res.: Oceans **113**: C03012. doi:10.1029/2007JC004217

Sastri, A. R., J. Gauthier, P. Juneau, and B. E. Beisner. 2014. Biomass and productivity responses of zooplankton communities to experimental thermocline deepening. Limnol. Oceanogr. **59**: 1–16. doi:10.4319/lo.2014.59.1.0001

Schindler, D. W., S. E. Bayley, B. R. Parker, K. G. Beaty, D. R. Cruikshank, E. J. Fee, E. U. Schindler, and M. P. Stainton. 1996. The effects of climatic warming on the properties of boreal lakes and streams at the Experimental Lakes area, northwestern Ontario. Limnol. Oceanogr. **41**: 1004–1017. doi:10.4319/lo.1996.41.5.1004

Schmale, O., J. Wäge, V. Mohrholz, N. Wasmund, U. Gräwe, G. Rehder, and N. Loick-Wilde. 2018. The contribution of zooplankton to methane supersaturation in the oxygenated upper waters of the Central Baltic Sea. Limnol. Oceanogr. **63**: 412–430. doi:10.1002/lno.10640

Schubert, C. J., F. Vazquez, T. Lösekann-Behrens, K. Knittel, M. Tonolla, and A. Boetius. 2011. Evidence for anaerobic oxidation of methane in sediments of a freshwater system (Lago di Cadagno). FEMS Microbiol. Ecol. **76**: 26–38. doi:10.1111/j.1574-6941.2010.01036.x

Sepúlveda Steiner, O., D. Bouffard, and A. Wüest. 2019. Convection-diffusion competition within mixed layers of stratified natural waters. Geophys. Res. Lett. **46**: 13199–13208. doi:10.1029/2019GL085361

Sepúlveda Steiner, O., D. Bouffard, and A. Wüest. 2021. Persistence of bioconvection-induced mixed layers in a stratified lake. Limnol. Oceanogr. **66**: 1531–1547. doi:10.1002/lno.11702

Solomon, C. T., and others. 2015. Ecosystem consequences of changing inputs of terrestrial dissolved organic matter to lakes: Current knowledge and future challenges. Ecosystems **18**: 376–389. doi:10.1007/s10021-015-9848-y

Sosa, O. A., D. J. Repeta, E. F. DeLong, M. D. Ashkezari, and D. M. Karl. 2019. Phosphate-limited ocean regions select for bacterial populations enriched in the carbon–phosphorus lyase pathway for phosphonate degradation. Environ. Microbiol. **21**: 2402–2414. doi:10.1111/1462-2920.14628

Stamatakis, A. 2014. RAxML version 8: a tool for phylogenetic analysis and post-analysis of large phylogenies. Bioinformatics **30**: 1312–1313. doi:10.1093/bioinformatics/btu033

Stawiarski, B., S. Otto, V. Thiel, U. Gräwe, N. Loick-Wilde, A. K. Wittenborn, and O. Schmale. 2019. Controls on zooplankton methane production in the central Baltic Sea. Biogeosciences **16**: 1–16. doi:10.5194/bg-16-1-2019

Steinle, L., and others. 2015. Water column methanotrophy controlled by a rapid oceanographic switch. Nat. Geosci. **8**: 378–382. doi:10.1038/ngeo2420

Su, G., J. Zopfi, H. Yao, L. Steinle, H. Niemann, and M. F. Lehmann. 2020. Manganese/iron-supported sulfate-dependent anaerobic oxidation of methane by archaea in lake sediments. Limnol. Oceanogr. **65**: 863–875. doi:10.1002/lno.11354

Taenzer, L., P. C. Carini, A. M. Masterson, B. Bourque, J. H. Gaube, and W. D. Leavitt. 2020. Microbial methane from methylphosphonate isotopically records source. Geophys. Res. Lett. **47**: e2019GL085872. doi:10.1029/2019GL085872

Tanentzap, A. J., and others. 2017. Terrestrial support of lake food webs: Synthesis reveals controls over cross-ecosystem resource use. Sci. Adv. **3**: e1601765. doi:10.1126/sciadv.1601765

Tang, K. W., K. M. L. Hutalle, and H. P. Grossart. 2006. Microbial abundance, composition and enzymatic activity during decomposition of copepod carcasses. Aquat. Microb. Ecol. **45**: 219–227. doi:10.3354/ame045219

Tang, K. W., M. I. Gladyshev, O. P. Dubovskaya, G. Kirillin, and H. P. Grossart. 2014. Zooplankton carcasses and non-predatory mortality in freshwater and inland sea environments. J. Plankton Res. **36**: 597–612. doi:10.1093/plankt/fbu014

Tang, K. W., D. F. McGinnis, D. Ionescu, and H. P. Grossart. 2016. Methane production in oxic lake waters potentially increases aquatic methane flux to air. Environ. Sci. Technol. Lett. **3**: 227–233. doi:10.1021/acs.estlett.6b00150

Teikari, J. E., D. P. Fewer, R. Shrestha, S. Hou, N. Leikoski, M. Mäkelä, and K. Sivonen. 2018. Strains of the toxic and bloom-forming *Nodularia spumigena* (cyanobacteria) can degrade methylphosphonate and release methane. ISME J. **12**: 1619–1630. doi:10.1038/s41396-018-0056-6

Traganza, E. D., J. W. Swinnerton, and C. H. Cheek. 1979. Methane supersaturation and ATP-zooplankton blooms in near-surface waters of the Western Mediterranean and the subtropical North Atlantic Ocean. Deep-Sea Res. Part A Oceanogr. Res. Pap. **26**: 1237–1245. doi:10.1016/0198-0149(79)90066-9

Venetz, J. 2019. Methane production through methylphosphonate decomposition as particularly important pathway in the methane cycle of Lake Cadagno. MSc. thesis. Univ. of Basel, Department Environmental Geosciences & Biogeochemistry.

Wang, Q., and others. 2021. Aerobic bacterial methane synthesis. Proc. Natl. Acad. Sci. USA **118**: e2019229118. doi:10.1073/pnas.2019229118

Wäge, J., and others. 2019. Microcapillary sampling of Baltic Sea copepod gut microbiomes indicates high variability among individuals and the potential for methane production. FEMS Microbiol. Ecol. **95**: fiz024. doi:10.1093/femsec/fiz024

Whitney, L. P., and M. W. Lomas. 2019. Phosphonate utilization by eukaryotic phytoplankton. Limnol. Oceanogr. Lett. **4**: 18–24. doi:10.1002/lol2.10100

Woolway, R. I., and C. J. Merchant. 2019. Worldwide alteration of lake mixing regimes in response to climate change. Nat. Geosci. **12**: 271–276. doi:10.1038/s41561-019-0322-x

Yao, M., C. Henny, and J. A. Maresca. 2016. Freshwater bacteria release methane as a by-product of phosphorus acquisition. Appl. Environ. Microbiol. **82**: 6994–7003. doi:10.1128/AEM.02399-16

Zhang, Y., and H. Xie. 2015. Photomineralization and photomethanification of dissolved organic matter in Saguenay River surface water. Biogeosciences **12**: 6823–6836. doi:10.5194/bg-12-6823-2015

Zhou, Y., and others. 2018. Accumulation of terrestrial dissolved organic matter potentially enhances dissolved methane levels in eutrophic Lake Taihu, China. Environ. Sci. Technol. **52**: 10297–10306. doi:10.1021/acs.est.8b02163

Acknowledgments

of the Alpine Biology Center Piora for maintaining the sampling platform on Lake Cadagno.

Conflict of Interest

None declared.